^{123}I-VIP binding. Whether this may be the case in all VIPomas, and whether all VIPomas can be detected by VIP scintigraphy remains unclear.

CONCLUSION

A small VIPoma was detected by ^{123}I-VIP scintigraphy before its successful surgical removal. We recommend VIP scintigraphy in VMS patients with tumor sites that are undetectable by conventional imaging before surgical intervention.

ACKNOWLEDGMENTS

The plasmids containing the receptor cDNAs for the human SSTRs 1 through 4 (pCMV-hSSTR 1, 3–4; phSSTR2) were provided by Dr. G. Bell (Howard Hughes Institute, Chicago, IL). The plasmid carrying the hSSTR5 was donated by Dr. A.M. O'Carroll (National Institutes of Health, Bethesda, MD). The clone phVIPR2 was provided by Dr. M. Svoboda (Universite Libre de Bruxelles, Brussels, Belgium) and the clone phIVR-8c (VIPR1) by Dr. A. Couvineau (Institute National de la Sante et de la Recherche Medicale, Paris, France).

REFERENCES

1. Verner JV, Morrison AB. Islet cell tumor and a syndrome of refractory watery diarrhea and hypokalemia. *Am J Med* 1958;25:374–380.
2. Said SI, Mutt V. Polypeptide with broad biological activity. Isolation from small intestine. *Science* 1970;169:1217–1218.
3. Mekhjian HS, O'Dorisio TM. VIPoma syndrome. *Semin Oncol* 1987;14:282–291.
4. Lamberts SWJ, Bakker WH, Reubi JC, Krenning EP. Somatostatin receptor imaging in the localization of endocrine tumors. *N Engl J Med* 1990;323:1246–1249.
5. Krenning EP, Kwekkeboom DJ, Pauwels S, Kvols K, Reubi R. Somatostatin receptor scintigraphy. *Nuclear Med Ann* 1995;20:716–731.
6. Virgolini I, Raderer M, Kurtaran A, et al. Iodine-123-vasoactive intestinal peptide for the localization diagnosis of intestinal adenocarcinomas and endocrine tumors. *N Engl J Med* 1994;331:1116–1121.
7. Virgolini I, Kurtaran A, Raderer M, et al. Vasoactive intestinal peptide receptor scintigraphy. *J Nucl Med* 1995;36:1732–1739.
8. Virgolini I, Yang Q, Li SR, et al. Cross-competition between vasoactive intestinal peptide (VIP) and somatostatin for binding to tumor cell receptors. *Cancer Res* 1994;54:690–700.
9. Sambrook J, Fritsch EF, Maniatis T, eds. *Molecular cloning*, 2nd ed. Cold Spring Harbor, NY: Cold Spring Harbor Laboratory Press; 1989:740.
10. McLeod MK, Few JW, Shapiro B. Diagnostic advances in APUDomas and other endocrine tumors: imaging and localization. *Semin Oncol* 1993;9:399–432.
11. Lamberts SWJ, Lely AJ, Herder WW, Hofland LJ. Octreotide. *N Engl J Med* 1996;334:246–254.

Indium-111-DTPA-Folate as a Potential Folate-Receptor-Targeted Radiopharmaceutical

Carla J. Mathias, Susan Wang, David J. Waters, John J. Turek, Philip S. Low and Mark A. Green

Departments of Medicinal Chemistry and Molecular Pharmacology, Chemistry, Veterinary Clinical Sciences and Veterinary Physiology and Pharmacology, Purdue University, West Lafayette, Indiana

Indium-111-labeled diethylenetriamine pentaacetic acid (DTPA)-folate was evaluated as a radiopharmaceutical for targeting tumor-associated folate receptors. **Methods:** Athymic mice were subcutaneously inoculated with ~1.8 × 10^6 folate receptor-positive KB (human nasopharyngeal carcinoma) cells, yielding 0.2- to 0.6-g tumors in 15 days, at which time ^{111}In-DTPA-folate, ^{111}In-DTPA or ^{111}In-citrate was administered by intravenous injection. **Results:** The ^{111}In-DTPA-folate conjugate afforded marked tumor-specific ^{111}In deposition in vivo using this mouse model. The involvement of the folate receptor in mediating tumor uptake of ^{111}In-DTPA-folate was demonstrated by the blocking of tumor uptake by coadministration of free folic acid (intravenous). The ^{111}In-DTPA-folate also shows folate receptor-mediated uptake and retention in the kidneys, presumably reflecting radiotracer binding to folate receptors of the proximal tubules. In control experiments, the ^{111}In-citrate radiopharmaceutical precursor was also shown to afford significant tumor uptake of ^{111}In, but with much poorer tumor-to-background tissue contrast than that obtained with ^{111}In-DTPA-folate. Unconjugated ^{111}In-DTPA showed no tumor affinity. **Conclusion:** Indium-111-DTPA-folate appears suitable as a radiopharmaceutical for targeting tumor-associated folate receptors.

Key Words: indium-111-diethylenetriamine pentaacetic acid folate; folate receptor; tumor targeting

J Nucl Med 1998; 39:1579–1585

The tumor cell membrane-associated folate receptor is a potential molecular target for selective radiopharmaceutical delivery to ovarian, endometrial and other human tumors known to overexpress folate-binding protein (FBP). The folate receptor is known to be overexpressed by a variety of neoplastic tissues, including breast, cervical, ovarian, colorectal, renal and nasopharyngeal tumors, while being highly restricted in most normal tissues (*1–10*). Previously, it has been shown that this receptor system can be targeted in vitro and in vivo with low molecular weight folate-chelate conjugates such as ^{67}Ga-deferoxamine-folate and ^{111}In-diethylenetriamine pentaacetic acid (DTPA)-folate (*11–15*). This study was undertaken to better characterize the ability of ^{111}In-DTPA-folate to target tumor folate receptors in vivo using an athymic mouse tumor model.

Received Jul. 11, 1997; revision accepted Dec. 19, 1997.

For correspondence or reprints contact: Mark A. Green, PhD, Professor of Medicinal Chemistry, Purdue University, 1333 Pharmacy Building, West Lafayette, IN 47907-1333.

MATERIALS AND METHODS

General

A Capintec CRC12R radionuclide dose calibrator (Capintec, Inc., Ramsey, NJ) was used for assays of ^{111}In radioactivity in the μCi-mCi range, whereas low-level (<0.01 μCi) samples of ^{111}In were counted in a Packard 5500 automatic gamma scintillation counter with a 3-in. large-bore NaI(Tl) crystal. Folate-deficient rodent chow was obtained from ICN Biomedicals (Costa Mesa, CA) and UV-irradiated before use. The DTPA-folate conjugate (Fig. 1) was prepared as described previously (*15*)

Preparation of Indium-111 Radiotracers

The ^{111}In-DTPA-folate conjugate, ^{111}In-DTPA and ^{111}In-citrate were prepared from no-carrier-added ^{111}In-indium(III)-chloride (Mallinckrodt, Inc., St. Louis, MO). Briefly, to prepare ^{111}In-DTPA-folate, the dilute HCl solution of $^{111}In^{3+}$ was buffered by addition of sodium citrate, followed by addition of an aqueous solution of the DTPA-folate ligand. Labeling was always complete

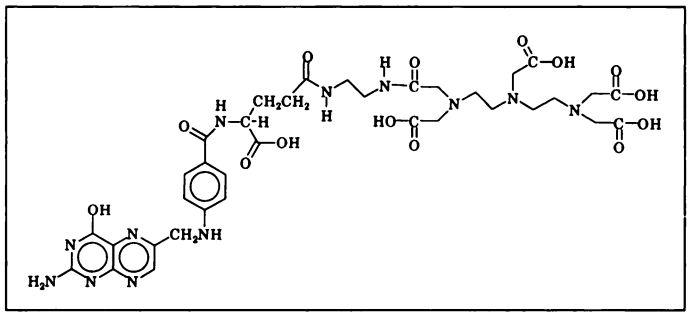

FIGURE 1. Structural formula of the DTPA-folate conjugate. In this conjugate, ethylenediamine serves as an amide-linked bridge between a DTPA carboxylate and the γ-carboxylate of folic acid.

after the reaction mixture was allowed to stand at room temperature for 2 hr. For control experiments, ^{111}In(III)-citrate was prepared by buffering the ^{111}In-chloride solution with 0.1–0.2 ml 3% sodium citrate (pH 7.4). A portion of the resulting ^{111}In-citrate solution (25–50 μl) was mixed with 0.15 mg DTPA to obtain ^{111}In-DTPA for further control experiments. The radiochemical purity of each ^{111}In-labeled compound was determined by thin-layer chromatography on C-18 reverse-phase plates developed with methanol and, in all cases, was found to exceed 90% at the time of use. Both ^{111}In-DTPA-folate and ^{111}In-DTPA migrate with R_f = 0.6–0.8, whereas the ^{111}In-citrate precursor remains at the origin (R_f = 0.0). All experiments using the ^{111}In-DTPA-folate tracer were performed within 1–3 days of radiolabeling; the radiochemical purity of the product was always reconfirmed by thin-layer chromatography before use.

Growth and Preparation of KB Cells

KB cells, a human nasopharyngeal epidermal carcinoma cell line that greatly overexpresses the FBP (*16,17*), were cultured in 75-cm^2 flasks continuously as a monolayer at 37°C in a humidified atmosphere containing 5% CO_2. Folate-deficient modified Eagle's medium (FDMEM) was used [a folate-free modified Eagle's medium purchased from Life Technologies, Inc. (Grand Island, NY) supplemented with 10% v/v heat-inactivated fetal calf serum as the only source of folate] containing penicillin (50 units/ml), streptomycin (50 μg/ml) and 2 m*M* L-glutamine. The final folate concentration in the complete FDMEM is ~3 n*M*, i.e., a value at the low end of the physiological concentration in human serum (*17,18*). For implantation, subconfluent KB cells were harvested by treatment with trypsin (140 USP units/ml) and EDTA (0.07 m*M*) in buffer (136.9 m*M* NaCl, 2.68 m*M* KCl, 8.1 m*M* Na_2HPO_4, 1.47 m*M* KH_2PO_4, and Phenol Red). The cells were then washed once with FDMEM and pelleted by spinning at 1000 × *g* for 3–5 min. The cell pellet was resuspended at 7.2 × 10^6 cells per 0.4 ml in FDMEM.

Athymic Mouse Tumor Model

Three- to 4-wk-old athymic mice (*nu/nu* strain) were purchased from Harlan Sprague Dawley, Inc. (Indianapolis, IN). All food, water and bedding were sterilized before use. Mice were housed under conditions of controlled temperature (72 ± 2°F) and humidity in polycarbonate cages using a microisolator system (Lab Products, Inc., Aberdeen, MD). Daily light cycles were 12 hr light/12 hr dark. After a 7-day acclimation period, the mice were inoculated subcutaneously with 0.1 ml tumor cell suspension (1.8 × 10^6 KB cells) into the interscapular region using a 25-gauge needle. All inoculations were performed within a laminar flow cabinet using aseptic technique. Subcutaneous tumor growth was monitored daily and radiotracer distribution studies were performed 15 days after tumor cell implantation. Unless otherwise indicated, animals used in the reported biodistribution experiments were exclusively fed folate-free rodent chow ad libitum for 21–23 days before radiopharmaceutical administration.

Imaging and Radiotracer Biodistribution Studies

The general procedure for the animal biodistribution studies has been described previously (*12*). Animals were anesthetized by inhalation of diethyl ether during radiotracer injections via the exposed femoral vein, as well as at the time of kill by decapitation. Syringes used for radiotracer injections were weighed on an analytical balance before and after injection to quantitate the dose received by each animal. The biodistribution of tracer in each sample was calculated as both a percentage of the injected dose (%ID) per organ and as a %ID/g of tissue wet weight, using reference counts from a weighed and appropriately diluted sample of the original injectate. Tumor-to-nontarget tissue ratios were calculated from the corresponding %ID/g values. A one-tailed Mann–Whitney test (*19*) was used to assess the significance of differences in radiotracer tumor uptake between groups of experimental animals in the reported biodistribution studies.

For gamma scintigraphy, mice were anesthetized with ketamine (40 mg/kg, intraperitoneally) and xylazine (4 mg/kg, intraperitoneally). Gamma images of intact animals were obtained using a Searle 37GP gamma scintillation camera fitted with a 300-keV parallel-hole collimator and linked to a Siemens MicroDELTA computer intravenous. Planar whole-body images were acquired at 5 hr (200,000-count image) and 24 hr (100,000-count image) after intravenous administration of ^{111}In-DTPA-folate (400 μCi ^{111}In; 85 μg DTPA-folate) to an athymic mouse (29.3 g) with subcutaneous human KB cell tumor (0.296 g). Shortly after ^{111}In-DTPA-folate administration, the animal was given 1.5 ml sterile saline by intraperitoneal injection to promote voiding of the urinary bladder before imaging.

Indium-111-DTPA-folate (~200 μCi/mouse; ~17 μg DTPA-folate per mouse) was administered intravenously to three tumor-bearing athymic mice under diethyl ether anesthesia. At 4 hr postinjection, the mice were anesthetized with ketamine (40 mg/kg, intraperitoneally) and xylazine (4 mg/kg, intraperitoneally) and whole-body perfusion performed through the left ventricle of the heart using a 4% paraformaldehyde-0.1% glutaraldehyde in 0.15 *M* Millonig's phosphate buffer. The kidneys were removed, and sections of kidney placed in fixative for an additional 30 min. The tissues were then rinsed in buffer, dehydrated through a graded ethanol gradient, rinsed two times in propylene oxide and embedded in epoxy resin (Poly/Bed 812; Polysciences, Inc., Warrington, PA). One-micron-thick sections of the kidney were placed onto silane-coated slides and stained using a periodic acid-iron hematoxylin stain. The slides were then dipped in Ilford L4 autoradiography emulsion that was diluted 1:1 with distilled water and warmed to 40°C. The slides were allowed to dry in the dark and placed in slide boxes containing silica gel desiccant at 4°C for 1–3 days. The slides were developed in undiluted Kodak D-19 developer at 4°C for 10 min, rinsed in water and then fixed in 24% sodium thiosulfate at 4°C. After rinsing in distilled water, slides were air-dried and coverslipped using Permount.

RESULTS

The primary model for evaluation of the biodistribution and pharmacokinetics of ^{111}In-DTPA-folate has been the athymic mouse bearing subcutaneously implanted folate-receptor-positive human KB cell tumors. Because normal rodent chow contains a high concentration of folic acid (6 mg/kg chow), the mice used in these receptor targeting studies were maintained on folate-free diet for 3 wk to achieve serum folate concentrations close to the range of normal human serum. After 3 wk on folate-free diet, mouse serum folate levels drop to 25 ± 7 n*M*

TABLE 1
Biodistribution of Indium-111-DTPA-Folate and Reference Tracers in Athymic Mice with Folate-Receptor-Positive KB Cell Tumors

	^{111}In %ID/g 4 hr after intravenous administration				
	^{111}In-DTPA-folate	^{111}In-DTPA-folate + folate coinjection*	^{111}In-DTPA-folate + folate chase at 3 hr†	^{111}In-DTPA‡	^{111}In-citrate
DTPA-folate dose (μmol/kg)	2.77 ± 0.35	2.78 ± 0.24	2.87 ± 0.25	—	—
Animal mass (g)	29.0 ± 3.6	29.5 ± 2.2	29.2 ± 1.1	28.5 ± 3.5	30.3 ± 2.5
Tumor mass (g)	0.33 ± 0.15	0.31 ± 0.11	0.31 ± 0.18	0.21 ± 0.08	0.44 ± 0.25
Blood	0.0093 ± 0.0029	0.20 ± 0.10	0.026 ± 0.008	0.0036 ± 0.0004	9.9 ± 2.3
Heart	0.032 ± 0.008	0.10 ± 0.04	0.033 ± 0.005	0.013 ± 0.001	3.7 ± 1.0
Lungs	0.048 ± 0.005	0.21 ± 0.09	0.050 ± 0.010	0.026 ± 0.001	6.5 ± 2.0
Liver	0.10 ± 0.02	2.8 ± 0.3	0.084 ± 0.013	0.084 ± 0.011	5.1 ± 1.3
Spleen	0.038 ± 0.011	0.58 ± 0.14	0.039 ± 0.002	0.024 ± 0.005	5.3 ± 1.8
Kidney	3.2 ± 0.6	31.2 ± 11.9	1.97 ± 0.15	0.85 ± 0.07	13.0 ± 1.3
Intestines and contents	0.45 ± 0.16	1.1 ± 0.5	0.38 ± 0.08	0.22 ± 0.13	3.3 ± 1.4
Muscle	0.094 ± 0.012	0.28 ± 0.08	0.059 ± 0.006	0.02 ± 0.01	1.6 ± 0.4
Tumor	3.1 ± 0.6	0.31 ± 0.13	2.38 ± 0.85	0.045 ± 0.005	3.6 ± 0.8
Tumor-to-blood§	346 ± 101	1.73 ± 0.45	96.8 ± 40.6	12.5 ± 0.5	0.38 ± 0.08
Tumor-to-liver§	31.1 ± 9.7	0.12 ± 0.06	28.8 ± 10.9	0.54 ± 0.02	0.72 ± 0.04
Tumor-to-kidney§	1.00 ± 0.34	0.010 ± 0.002	1.22 ± 0.46	0.05 ± 0.01	0.28 ± 0.07
Tumor-to-muscle§	33.3 ± 9.8	1.10 ± 0.23	41.4 ± 17.6	2.4 ± 0.5	2.4 ± 0.4

*Folate (205 ± 18 μmol/kg) coinjected with ^{111}In-DTPA-folate.
†Folate chase (203 ± 24 μmol/kg) administered by intravenous injection 188 ± 10 min after administration of ^{111}In-DTPA-folate.
‡n = 3.
§Tumor-to-background tissue ratios based on corresponding %ID/g data.
Values shown represent the mean ± s.d. of data from four animals (n = 3 for In-DTPA).

from the initial 720 ± 260 n*M* serum folate level when the animals were fed normal rodent chow (*12*). This dietary intervention is believed to be a reasonable manipulation of the animal model because the mice would have serum folate levels that were only slightly higher than the 9–14 n*M* folate concentration of normal human serum (*18*). Thus, in these mouse biodistribution studies, the ^{111}In-DTPA-folate is competing for tumor folate receptors against physiologically relevant concentrations of endogenous serum folate.

In an initial study to evaluate the ability of ^{111}In-DTPA-folate to target folate receptors in vivo, three groups of four tumor-bearing mice received the ^{111}In-DTPA-folate conjugate intravenously. To competitively block the folate receptor, one group of mice receiving ^{111}In-DTPA-folate also received simultaneously an intravenous dose of folic acid. To allow examination of competitive displacement of the ^{111}In-DTPA-folate radiotracer, one group of mice receiving ^{111}In-DTPA-folate subsequently received a chase dose of folic acid (intravenously) 3 hr after the ^{111}In-DTPA-folate administration. A fourth group of animals (n = 3) received unconjugated ^{111}In-DTPA intravenously and, as an additional control experiment, a fifth group of animals (n = 4) received ^{111}In-citrate intravenously. All animals in this study were killed by decapitation 4 hr following radiotracer administration and the tissue uptake of radiotracer quantitated (Table 1). The tumor uptake of radiotracer obtained with ^{111}In-DTPA-folate, ^{111}In-DTPA, and ^{111}In-citrate was reasonably reproducible within the groups of mice, whereas clear variations were apparent between groups (Fig. 2 and Table 1).

The ^{111}In-DTPA-folate tracer was found to significantly concentrate in the folate receptor-bearing KB tumors (Table 1 and Fig. 2) with tumor uptake of 1.0% ± 0.5% of the injected dose (3.1% ± 0.6%ID/g) at 4 hr postinjection. Excellent tumor-to-blood, tumor-to-liver and tumor-to-muscle contrast

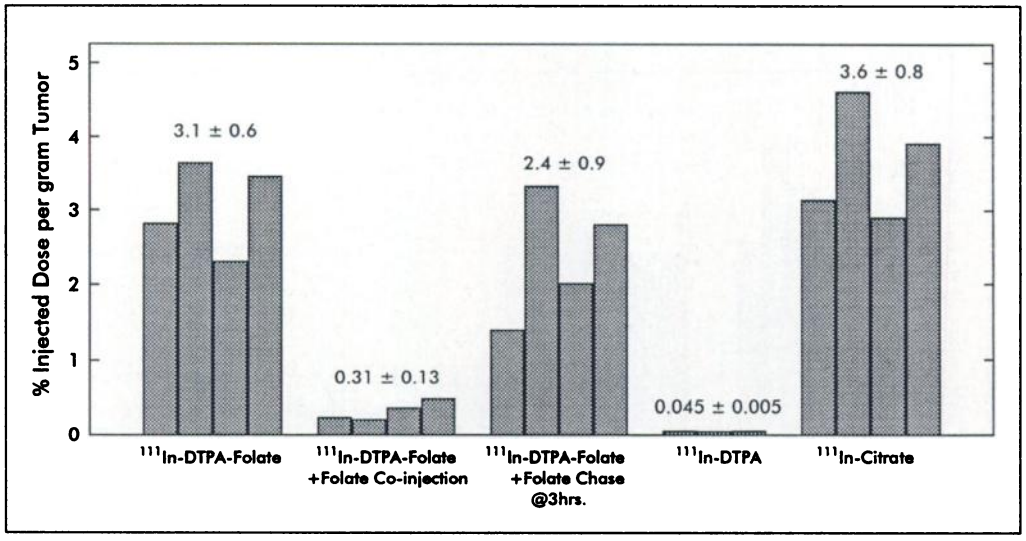

FIGURE 2. Tumor uptake of ^{111}In-DTPA-folate, ^{111}In-DTPA and ^{111}In-citrate in mice with folate-receptor-positive KB cell tumors. Each column represents data from one animal. The mean tumor uptake (± s.d.) is shown above the data for each group of animals.

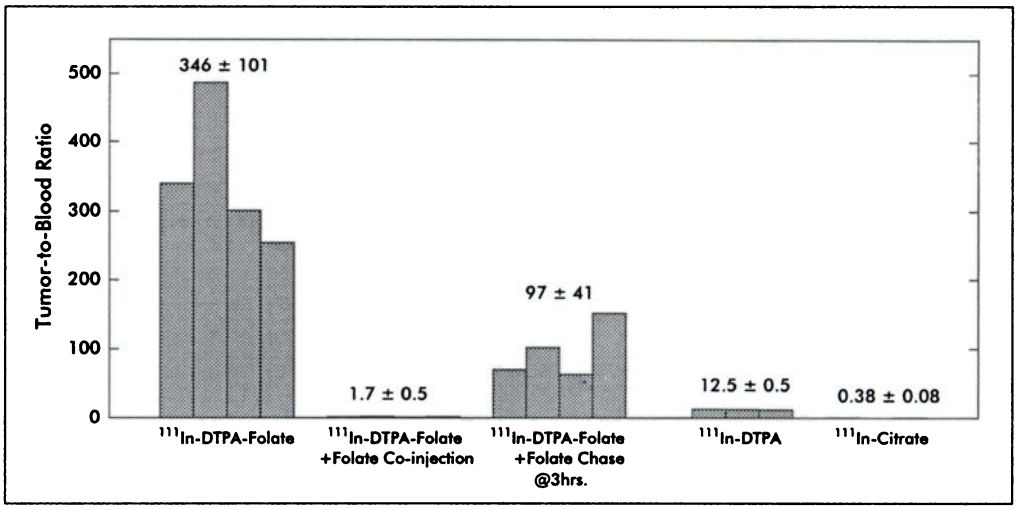

FIGURE 3. Tumor-to-blood ratios after intravenous administration of ^{111}In-DTPA-folate, ^{111}In-DTPA or ^{111}In-citrate to mice with KB cell tumors. Each column represents the data from one animal. The mean tumor-to-blood ratio (± s.d.) is shown above the data for each group of animals.

was observed with the four animals that received ^{111}In-DTPA-folate alone, where the tumor-to-blood, tumor-to-liver and tumor-to-muscle ratios were 346 ± 101, 31.1 ± 9.7 and 33.3 ± 9.8, respectively. Tumor-to-intestine contrast obtained with ^{111}In-DTPA-folate was better than that previously observed with ^{67}Ga-deferoxamine-folate (*12,13*), due to more efficient renal clearance of the ^{111}In tracer and a corresponding decrease in the fraction of ^{111}In cleared into the intestines through the hepatobiliary system.

The specific involvement of the folate receptor in mediating tumor uptake of ^{111}In-DTPA-folate is demonstrated by the 10-fold reduction of tumor radiotracer accumulation in mice that received ^{111}In-DTPA-folate with a simultaneous blocking dose of folic acid ($p \leq 0.05$) (Table 1 and Fig. 2). This contrasts with the behavior of ^{111}In-DTPA-folate in animals that received a "chase" dose of folic acid (intravenously) 3 hr after radiotracer injection, where tumor uptake of ^{111}In is only slightly reduced from 3.1 ± 0.6 to 2.4% ± 0.9%ID/g, suggesting that tumor-localized ^{111}In tracer had largely been internalized by the tumor cells. Control experiments demonstrated that, as expected, unconjugated ^{111}In-DTPA has no tumor affinity (Table 1 and Figs. 2 and 3). The ^{111}In-citrate synthetic precursor does itself show tumor affinity (presumably mediated via ^{111}In-transferrin) but provides much poorer tumor-to-background tissue contrast (Table 1 and Figs. 2 and 3).

To better characterize the ability of ^{111}In-DTPA-folate to target tumor folate receptors, the indicator-dilution method was used to demonstrate that tumor uptake of radiotracer behaves as expected for a receptor-mediated process. The ^{111}In-DTPA-folate radiopharmaceutical (44 nmol DTPA-folate/kg) was administered (intravenously) with varying blocking doses of folic acid (0.0, 0.31, 3.2, 32 or 320 μmol/kg) to mice bearing the folate-receptor-positive human KB cell tumors. The tumor uptake of ^{111}In-DTPA-folate at 4 hr was found to vary in a dose-dependent fashion, dropping from 6.9% ± 1.7%ID/g at the highest effective specific activity to 1.1% ± 0.2%ID/g when administered with 320 μmol/kg competing folic acid (Fig. 4 and Table 2). Thus, the unlabeled free folic acid does appear to effectively compete with ^{111}In-DTPA-folate for occupancy of tumor receptor sites.

Retention of ^{111}In in the kidney was also found to vary in a dose-dependent fashion, presumably reflecting radiotracer binding to folate receptors known to be present in the proximal tubules (*20–24*). This interpretation is supported by a micro-autoradiographic study of kidney slices that shows the renal-associated ^{111}In-radiotracer to be selectively localized in the proximal tubules (Fig. 5). Four-hour kidney levels of ^{111}In progressively drop as the dose of free folic acid increased from 0.0 μmol/kg to 0.31 μmol/kg and 3.3 μmol/kg (Table 2). This finding is consistent with competitive folate receptor binding by folic acid. However, the kidney uptake of ^{111}In then paradoxically rises at the higher 32 μmol/kg and 320 μmol/kg folic acid doses. The latter dose-dependent increase in renal levels of ^{111}In is believed to artifactually result from mechanical obstruction of the collecting system as folic acid is concentrated and acidified in the urine (analogous to the known tendency of similarly soluble antifolates, such as methotrexate, to precipitate in the collecting system as urine is concentrated and acidified) (*25*).

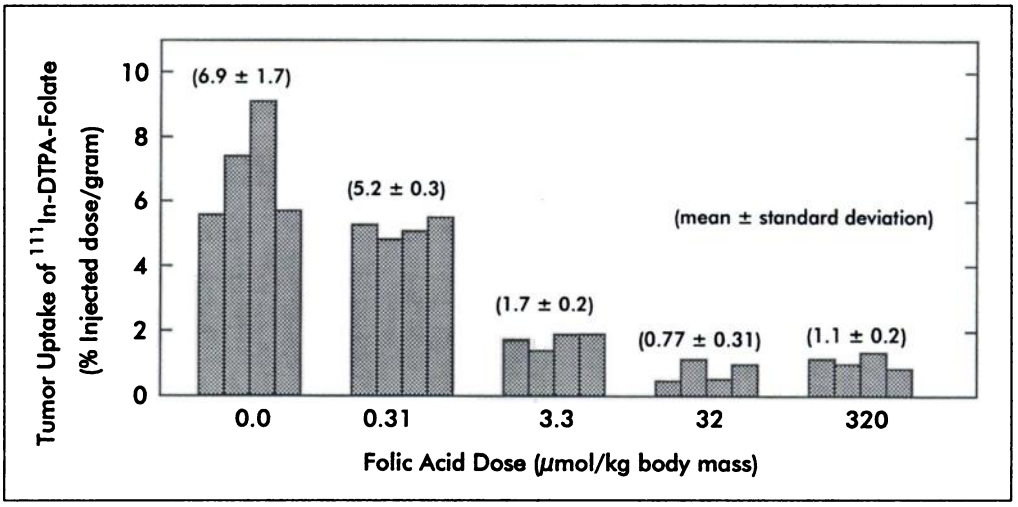

FIGURE 4. Bar graph illustrating that tumor uptake of ^{111}In-DTPA-folate is competitively blocked by coinjection of free folic acid. Data shown is from athymic mice bearing folate-receptor-positive KB cell tumors. Each column represents data from one animal. All animals were killed 4 hr following intravenous administration of the radiotracer. For all animals, the dose of DTPA-folate conjugate was 44 nmol/kg.

TABLE 2
Biodistribution of Indium-111-Diethylenetriamine Pentaacetic Acid (DTPA)-Folate in Athymic Mice with Folate-Receptor-Positive KB Cell Tumors: Dose Escalation Study

	^{111}In %ID/g 4 hr after intravenous administration				
	A ^{111}In-DTPA-folate	B ^{111}In-DTPA-folate + folic acid	C ^{111}In-DTPA-folate + folic acid	D ^{111}In-DTPA-folate + folic acid	E ^{111}In-DTPA-folate + folic acid
Folic acid dose (μmol/kg)	0 ± 0	0.305 ± 0.024	3.29 ± 0.28	32.2 ± 1.6	321 ± 47
DTPA-folate dose (nmol/kg)	46.9 ± 3.7	41.2 ± 3.3	44.4 ± 3.8	43.4 ± 2.2	43.5 ± 6.4
Animal mass (g)	27.2 ± 1.7	27.6 ± 4.6	29.1 ± 2.3	29.9 ± 1.4	28.9 ± 2.1
Tumor mass (g)	0.38 ± 0.19	0.60 ± 0.21	0.55 ± 0.14	0.69 ± 0.06	0.57 ± 0.22
Blood	0.062 ± 0.009	0.025 ± 0.003	0.021 ± 0.002	0.40 ± 0.29	1.05 ± 0.26
Heart	1.4 ± 0.2	0.069 ± 0.009	0.033 ± 0.016	0.18 ± 0.12	0.44 ± 0.12
Lungs	0.94 ± 0.17	0.077 ± 0.018	0.057 ± 0.016	0.38 ± 0.22	0.89 ± 0.24
Liver	1.82 ± 0.26	0.16 ± 0.02	0.14 ± 0.08	0.49 ± 0.21	0.80 ± 0.21
Spleen	0.28 ± 0.06	0.060 ± 0.009	0.058 ± 0.034	0.25 ± 0.11	0.52 ± 0.12
Kidney	82.1 ± 8.5	15.5 ± 0.8	2.6 ± 0.2	43.5 ± 14.1	102.0 ± 4.7
Intestines and contents	0.98 ± 0.20	0.43 ± 0.06	0.54 ± 0.08	1.7 ± 0.4	1.4 ± 0.3
Muscle	2.3 ± 0.3	0.15 ± 0.02	0.068 ± 0.035	0.29 ± 0.12	0.94 ± 0.07
Testes	1.49 ± 0.38	0.25 ± 0.03	0.072 ± 0.015	0.21 ± 0.08	0.35 ± 0.09
Tumor	6.93 ± 1.66	5.16 ± 0.28	1.74 ± 0.23	0.77 ± 0.34	1.08 ± 0.22
Tumor-to-blood*	114 ± 32	210 ± 32	82 ± 15	2.4 ± 0.9	1.0 ± 0.1
Tumor-to-liver*	3.9 ± 1.3	32.9 ± 4.3	15.1 ± 6.1	1.58 ± 0.15	1.37 ± 0.15
Tumor-to-kidney*	0.085 ± 0.021	0.33 ± 0.03	0.68 ± 0.13	0.017 ± 0.003	0.011 ± 0.003
Tumor-to-muscle*	3.1 ± 0.7	35.7 ± 4.9	30.8 ± 16.4	2.68 ± 0.75	1.14 ± 0.16

*Tumor-to-background tissue ratios based on corresponding %ID/g data.
Values shown represent the mean ± s.d. of data from four animals.

Renal folate receptors appear to be blocked at lower folate doses than those required to saturate radiotracer uptake by tumor cells, presumably because the receptors of the proximal tubule are exposed to a higher fraction of the injected dose as material clears into the urine. Thus, optimal tumor-to-kidney contrast occurred at the intermediate dosage of competing folic acid (3.2 μmol/kg), where ^{111}In-DTPA-folate provided tumor uptake of 1.7% ± 0.2%ID/g and tumor-to-blood, tumor-to-liver, tumor-to-muscle and tumor-to-kidney ratios of 82 ± 15, 15 ± 6, 31 ± 16 and 0.68 ± 0.13, respectively (Table 2).

Somewhat elevated ^{111}In uptake was observed in heart, lungs, liver, spleen, muscle and testes, when ^{111}In-DTPA-folate was administered at the highest effective specific activity (Table 2, Group A). This may be due to radiotracer binding to folate receptors associated with these normal tissues, because they exhibited a 5- to 20-fold decrease in ^{111}In uptake when the radiotracer was coinjected with folic acid at a dose of 0.31 μmol/kg (Group B). The slight rise in normal tissue uptake of ^{111}In at the highest folic acid doses (Groups D and E) is probably an artifact of the radiotracer's dramatically altered renal handling and excretion kinetics in those animals.

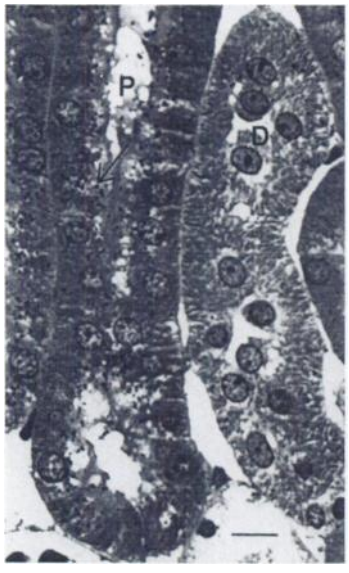

FIGURE 5. Autoradiograph of kidney from mouse receiving ~200 μCi of ^{111}In-DTPA-folate. This 1-μm-thick plastic section contains a portion of a proximal convoluted tubule (P) and a distal convoluted tubule (D). The silver grains (arrow) were localized exclusively to the proximal convoluted tubule. Bar = 10 μm.

To better define the time course of ^{111}In-DTPA-folate localization in folate-receptor-positive KB cell tumors, as well as to provide data for estimation of the radiation absorbed dose that could be expected from use of ^{111}In-DTPA-folate to image folate receptors in humans, a third animal study focused on determination of how ^{111}In-DTPA-folate biodistribution varied as a function of time (Table 3). For this pharmacokinetic study, the ^{111}In-DTPA-folate (35 nmol DTPA-folate/kg) was coadministered with folic acid at a dose (0.36 μmol/kg) that was previously shown to provide reasonable tumor-to-background contrast (Table 2).

The tumor uptake of ^{111}In (expressed as a %ID/g) was found to increase from 1 to 30 min after ^{111}In-DTPA-folate injection but then essentially remained stable from 30 min to 24 hr postinjection. Specifically, the tumor uptakes of ^{111}In-DTPA at 1 min, 5 min, 30 min, 1 hr, 2 hr, 4 hr, 24 hr and 48 hr postinjection were: 3.9 ± 2.0, 3.9 ± 0.8, 6.3 ± 1.7, 5.8 ± 1.3, 6.9 ± 0.9, 7.3 ± 1.8, 5.8 ± 1.9 and 3.9% ± 0.5%ID/g, respectively (n = 4). As in the previous biodistribution studies, a fraction of the radiotracer cleared from blood by the kidneys was not efficiently excreted into the urine, again apparently due to radiotracer binding to folate receptors of the proximal tubule. However, renal radioactivity at the observed levels (Table 3) may not be prohibitive for human studies. No tissues other than tumor and kidney showed appreciable concentration of the ^{111}In radiolabel after intravenous administration of ^{111}In-DTPA-folate. The uptake and retention of ^{111}In-DTPA-folate by tumor and kidney, as well as the lack of appreciable radiotracer concentration in other body tissues, are also qualitatively apparent in whole-body gamma images obtained at 5 and 24 hr

TABLE 3
Biodistribution of Indium-111-DTPA-Folate in Athymic Mice with Folate Receptor-Positive KB Cell Tumors

	^{111}In %ID/g after intravenous administration							
	1 min	5 min	30 min	1 hr	2 hr	4 hr	24 hr	48 hr
Dose folic acid dihydrate* (μg/kg)	167 ± 26	176 ± 19	172 ± 18	189 ± 20	164 ± 25	152 ± 21	173 ± 20	175 ± 13
Dose DTPA-folate (μg/kg)	29.7 ± 4.5	31.3 ± 3.3	30.4 ± 3.1	33.6 ± 3.5	29.2 ± 4.5	26.9 ± 3.7	30.7 ± 3.6	31.1 ± 2.3
Animal mass (g)	26.16 ± 3.28	25.44 ± 2.11	25.21 ± 1.85	24.66 ± 2.98	26.87 ± 3.05	26.23 ± 1.46	24.75 ± 1.97	24.73 ± 1.22
Tumor mass (g)	0.19 ± 0.13	0.29 ± 0.10	0.13 ± 0.04	0.23 ± 0.05	0.25 ± 0.09	0.25 ± 0.24	0.27 ± 0.07	0.29 ± 0.27
Blood	12.7 ± 0.7	6.3 ± 0.7	0.56 ± 0.18	0.094 ± 0.028	0.031 ± 0.006	0.024 ± 0.006	0.015 ± 0.004	0.0068 ± 0.0018
Heart	4.2 ± 0.2	2.2 ± 0.2	0.25 ± 0.07	0.068 ± 0.012	0.044 ± 0.012	0.051 ± 0.013	0.037 ± 0.003	0.036 ± 0.009
Lungs	8.8 ± 1.3	4.4 ± 0.5	0.70 ± 0.09	0.19 ± 0.05	0.077 ± 0.047	0.069 ± 0.008	0.041 ± 0.003	0.032 ± 0.002
Liver	3.3 ± 0.2	1.9 ± 0.3	0.53 ± 0.07	0.31 ± 0.04	0.45 ± 0.52	0.12 ± 0.05	0.077 ± 0.003	0.068 ± 0.020
Spleen	2.9 ± 0.4	1.5 ± 0.3	0.19 ± 0.04	0.060 ± 0.010	0.054 ± 0.007	0.046 ± 0.004	0.042 ± 0.004	0.041 ± 0.021
Kidney (1)	39.7 ± 9.6	17.9 ± 4.4	9.4 ± 0.5	7.6 ± 1.4	9.6 ± 1.9	10.3 ± 0.7	7.8 ± 1.1	6.1 ± 0.9
Adrenal (1)	4.3 ± 1.0	1.7 ± 0.4	0.53 ± 0.25	0.32 ± 0.12	0.25 ± 0.18	0.47 ± 0.11	0.23 ± 0.14	0.17 ± 0.05
Stomach	2.3 ± 0.9	1.14 ± 0.29	0.30 ± 0.06	0.084 ± 0.035	0.040 ± 0.021	0.052 ± 0.023	0.053 ± 0.020	0.035 ± 0.015
Intestines	2.9 ± 0.4	1.6 ± 0.3	0.42 ± 0.06	0.35 ± 0.04	0.50 ± 0.31	0.42 ± 0.10	0.16 ± 0.05	0.063 ± 0.011
Pancreas	2.1 ± 0.1	1.28 ± 0.21	0.22 ± 0.05	0.069 ± 0.016	0.058 ± 0.016	0.054 ± 0.018	0.046 ± 0.008	0.041 ± 0.009
Ovary (1)	2.1 ± 0.5	2.16 ± 0.89	0.48 ± 0.15	0.16 ± 0.03	0.18 ± 0.06	0.22 ± 0.07	0.12 ± 00.68	0.16 ± 0.02
Uterus	6.0 ± 2.9	4.6 ± 0.95	0.57 ± 0.14	0.16 ± 0.03	0.14 ± 0.04	0.15 ± 0.03	0.14 ± 0.072	0.14 ± 0.08
Red muscle	1.7 ± 0.2	1.3 ± 0.3	0.16 ± 0.03	0.089 ± 0.094	0.039 ± 0.017	0.028 ± 0.005	0.0095 ± 0.0020	0.021 ± 0.010
White muscle	2.1 ± 0.3	2.2 ± 0.5	0.32 ± 0.07	0.078 ± 0.023	0.059 ± 0.013	0.064 ± 0.021	0.039 ± 0.006	0.051 ± 0.012
Skin	3.9 ± 0.7	4.7 ± 0.6	0.77 ± 0.32	0.24 ± 0.07	0.18 ± 0.05	0.20 ± 0.06	0.14 ± 0.01	0.12 ± 0.02
Bone (femur)	2.3 ± 0.4	—	—	0.063 ± 0.014	—	—	0.054 ± 0.021	0.037 ± 0.015
Bone (tibia)	2.1 ± 0.3	—	—	0.071 ± 0.034	—	—	0.051 ± 0.007	0.038 ± 0.006
Brain	0.4 ± 0.1	0.22 ± 0.02	0.06 ± 0.01	0.040 ± 0.004	0.051 ± 0.004	0.047 ± 0.007	0.035 ± 0.005	0.032 ± 0.010
Bladder and contents	7.2 ± 3.6	22.8 ± 12.7	2.17 ± 0.80	0.69 ± 0.18	9.3 ± 17.8	0.26 ± 0.12	0.32 ± 0.08	0.15 ± 0.02
Tumor	3.9 ± 2.0	3.9 ± 0.8	6.34 ± 1.74	5.82 ± 1.32	6.87 ± 0.93	7.25 ± 1.82	5.79 ± 1.90	3.87 ± 0.53
Tumor-to-blood†	0.31 ± 0.15	0.63 ± 0.15	12.1 ± 4.6	69.8 ± 39.7	227 ± 64	301 ± 65	384 ± 48	604 ± 183
Tumor-to-liver†	1.19 ± 0.56	2.15 ± 0.55	12.0 ± 3.2	19.7 ± 7.3	29.5 ± 18.9	69 ± 37	75 ± 23	62.4 ± 23.6
Tumor-to-kidney†	0.10 ± 0.06	0.23 ± 0.07	0.67 ± 0.16	0.79 ± 0.29	0.74 ± 0.20	0.71 ± 0.20	0.75 ± 0.25	0.65 ± 0.15
Tumor-to-muscle†	2.4 ± 1.3	3.13 ± 0.96	38.8 ± 8.5	118 ± 67	197 ± 67	269 ± 90	646 ± 324	247 ± 194

*Formula weight of folic acid dihydrate = 477 Da; molecular weight of DTPA-folic acid conjugate = 859 Da.
†Tumor-to-background ratios based on corresponding %ID/data.
Values shown represent the mean ± s.d. of data from four animals.

following administration of ^{111}In-DTPA-folate to a mouse with folate-receptor-positive tumor (Fig. 6).

DISCUSSION

The ^{111}In-DTPA-folate radiopharmaceutical targets a cell membrane folate receptor or FBP that is known to be overexpressed by several tumor cell types (e.g., ovarian, cervical, breast, colorectal, renal and nasopharyngeal tumors), while being highly restricted in normal tissues (*1–10,26–31*). A few normal tissues, such as the choroid plexus, placenta and proximal tubules of the kidney, do express low concentrations of the folate receptor, with very low levels also found in lung and thyroid (*4,5,9,26*). Folate-binding protein is so dramatically overexpressed in many tumors that this receptor has been exploited in vitro as a marker to localize and visualize tumor cells (*3*). Many tumor-specific monoclonal antibodies with previously unidentified antigen targets have been recently shown to simply recognize FBP (*2,3,5,6,26–30*). The ability of ^{111}In-DTPA-folate to target the folate receptor in vitro has been described using cultured human tumor cells (*15*).

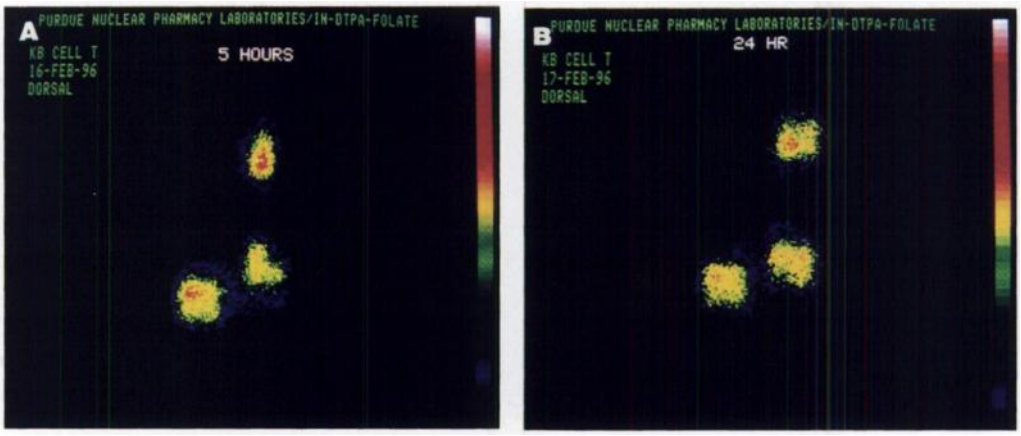

FIGURE 6. Whole-body gamma images (dorsal view) obtained at 5 hr (A) and 24 hr (B) following intravenous administration of ^{111}In-DTPA-folate to a mouse with subcutaneous folate-receptor-positive KB cell tumor in the right shoulder. Only the kidneys (lower pair of hot spots) and tumor (upper hot spot) exhibit significant accumulation of radiotracer.

Two folate receptor isoforms are known, FR-alpha and FR-beta (*9*). These differ in their tissue distribution, stereospecificity and relative affinity for folates (9). The tumor-associated folate receptor of ovarian carcinoma and KB cells is the FR-alpha isoform (*9,31*), which has the higher folate binding affinity, whereas the FR-beta isoform is more common in normal tissues (*9*).

This study demonstrates in an athymic mouse model that ^{111}In-DTPA-folate is able to selectively target folate receptor-positive tumors, providing significant tumor uptake and retention of the radiolabel. Involvement of the folate receptor in mediating tumor accumulation of ^{111}In-DTPA-folate is confirmed by the competitive blocking observed when radiotracer was coadministered with varying amounts of folic acid (Fig. 4 and Table 2). The ^{111}In-DTPA-folate radiopharmaceutical was found to provide excellent tumor-to-nontarget tissue contrast for all tissues except the kidney (Fig. 6 and Tables 2 and 3), where folate receptors of the proximal tubules afford tracer uptake and retention that equals or exceeds that observed in the folate-receptor-positive tumors. Because it is not known how renal folate receptor concentrations vary between species, it remains unclear whether renal uptake of ^{111}In-DTPA-folate will be a prohibitive problem in humans.

An area where such a folate-receptor-targeted imaging agent could have clinical impact is in the diagnosis and management of patients with ovarian cancer. The folate receptor appears to be overexpressed by >90% of both ovarian and endometrial carcinomas (*6,31*), making these tumors excellent candidates for imaging with a folate-receptor-targeted radiopharmaceutical such as ^{111}In-DTPA-folate. In addition, ovarian cancer is a disease in which noninvasive tumor detection with high sensitivity and specificity might improve the quality of patient care, due to:

1. The high probability of Stage III or IV disease with distant metastasis at the time of presentation;
2. The importance of cytoreductive surgery in patient management; and
3. The limited ability of alternative imaging modalities (MRI, CT and ultrasound) to rule out disease recurrence (*32*).

In the case of ^{111}In-DTPA-folate, it remains necessary to define how well radiopharmaceutical performance in humans can be predicted by the tumor mouse data.

CONCLUSION

The available animal results demonstrate the feasibility of targeting folate receptors with ^{111}In-DTPA-folate in vivo. The ^{111}In-DTPA-folate radiopharmaceutical is rapidly cleared from the blood after intravenous administration and is excreted primarily in the urine. In athymic mice bearing folate receptor-positive KB cell tumors, tumor and the kidneys are the only tissues that selectively concentrate and retain the receptor-targeted ^{111}In radiolabel. The receptor-based tumor targeting observed with ^{111}In-DTPA-folate suggests that this radiopharmaceutical may be useful in humans for noninvasive imaging of folate receptor-positive tumors.

ACKNOWLEDGMENTS

This work was supported in part by National Cancer Institute (National Institutes of Health) Grant R01-CA70845, as well as a financial gift from Endocyte, Inc. The Purdue Athymic Mouse Facility is partially supported by Cancer Center (Core) Support Grant P30-CA23168.

REFERENCES

1. Rettig W, Garin-Chesa P, Beresford H, Oettgen H, Melamed M, Old L. Cell-surface glycoproteins of human sarcomas: differential expression in normal and malignant tissues and cultured cells. *Proc Natl Acad Sci USA* 1988;85:3110–3114.
2. Campbell IG, Jones TA, Foulkes WD, Trowsdale J. Folate-binding protein is a marker for ovarian cancer. *Cancer Res* 1991;51:5329–5338.
3. Coney LR, Tomassetti A, Carayannopoulos L, et al. Cloning of a tumor-associated antigen: MOv18 and MOv19 antibodies recognize a folate-binding protein. *Cancer Res* 1991;51:6125–6132.
4. Stein R, Goldenberg DM, Mattes J. Normal tissue reactivity of four anti-tumor monoclonal antibodies of clinical interest. *Int J Cancer* 1991;47:163–169.
5. Weitman SD, Lark RH, Coney LR, et al. Distribution of the folate receptor (GP38) in normal and malignant cell lines and tissues. *Cancer Res* 1992;52:3396–3401.
6. Garin-Chesa P, Campbell I, Saigo P, Lewis J, Old L, Rettig W. Trophoblast and ovarian cancer antigen LK26. Sensitivity and specificity in immunopathology and molecular identification as a folate-binding protein. *Am J Pathol* 1993;142:557–567.
7. Holm J, Hansen SI, Sondergaard K, Hoier-Madsen M. The high affinity folate binding protein in normal and malignant mammary gland tissue. *Chem Biol Pteridines Folates* 1993:757–760.
8. Franklin WA, Waintrub M, Edwards D, et al. New anti-lung-cancer antibody cluster 12 reacts with human folate receptors present on adenocarcinoma. *Int J Cancer* 1994; 8(suppl):89–95.
9. Ross JF, Chaudhuri PK, Ratnam M. Differential regulation of folate receptor isoforms in normal and malignant tissues in vivo and in established cell lines. Physiologic and clinical implications. *Cancer* 1994;73:2432–2443.
10. Li PY, Del Vecchio S, Fonti R, et al. Local concentration of folate binding protein GP38 in sections of human ovarian carcinoma by in vitro quantitative autoradiography. *J Nucl Med* 1996;37:665–672.
11. Wang S, Lee RJ, Mathias CJ, Green MA, Low PS. Synthesis, purification, and tumor cell uptake of ^{67}Ga-deferoxamine-folate, a potential radiopharmaceutical for tumor imaging. *Bioconj Chem* 1996;7:56–62.
12. Mathias CJ, Wang S, Lee RJ, Waters DJ, Low PS, Green MA. Tumor selective radiopharmaceutical targeting via receptor-mediated endocytosis: evaluation of a gallium-67 labeled deferoxamine-folate conjugate. *J Nucl Med* 1996;37:1003–1008.
13. Mathias CJ, Wang S, Waters DJ, Low PS, Green MA. Ga-67 and In-111 labeled folate-chelate conjugates for targeting tumor-associated folate binding protein [Abstract]. *J Nucl Med* 1996;37:347P–348P.
14. Mathias CJ, Wang S, Waters DJ, Turek JJ, Low PS, Green MA. Indium-111-DTPA-folate as a radiopharmaceutical for targeting tumor-associated folate-binding protein [Abstract]. *J Nucl Med* 1997;38:133P–134P.
15. Wang S, Luo J, Lantrip DA, et al. Design and synthesis of ^{111}In-DTPA-folate for use as a tumor-targeted radiopharmaceutical. *Bioconj Chem* 1997;8:673–679.
16. McHugh M, Cheng YC. Demonstration of a high affinity folate binder in human cell membranes and its characterization in cultured human KB cells. *J Biol Chem* 1979;254:11312–11318.
17. Antony AC, Kane MA, Portillo RM, Elwood PC, Kolhouse JF. Study of the role of a particulate folate-binding protein in the uptake of 5-methyltetrahydrofolate. *J Biol Chem* 1985;260:14911–14917.
18. Kutsky RJ. *Handbook of vitamins, minerals, and hormones*, 2nd ed. New York: Van Nostrand Reinhold; 1981:273.
19. Samuels ML. *Statistics for the life sciences*. San Francisco; Dellen; 1989:249–256.
20. Selhub J, Franklin WA. The folate-binding protein of rat kidney. *J Biol Chem* 1984;259:6601–6606.
21. Selhub J, Emmanouel D, Stavropoulos T, Arnold R. Renal folate absorption and the kidney folate binding protein. I. Urinary clearance studies. *Am J Physiol* 1987;252: F750–F756.
22. Selhub J, Nakamura S, Carone FA. Renal folate absorption and the kidney folate binding protein. II. Microinfusion studies. *Am J Physiol* 1987;252:F757–F760.
23. Williams WM, Huang KC. Renal tubular transport of folic acid and methotrexate in the monkey. *Am J Physiol* 1982;242:F484–F490.
24. Birn H, Nielsen S, Christensen EI. Internalization and apical-to-basolateral transport of folate in rat kidney proximal tubule. *Am J Physiol* 1997;272:F70–F78.
25. Crom WR, Evans WE. Methotrexate. In: Evans WE, Schentag JJ, Jusko WJ, Relling MV, eds. *Applied pharmacokinetics*, 3rd ed. Vancouver, WA: Applied Therapeutics; 1992:29-1–29-42.
26. Miotti S, Canevari S, Menard S, et al. Characterization of human ovarian carcinoma-associated antigens defined by novel monoclonal antibodies with tumor-restricted specificity. *Int J Cancer* 1987;39:297–303.
27. Mezzanzanica D, Garrido MA, Neblock DS, et al. Human T-lymphocytes targeted against an established human ovarian carcinoma with a bispecific F(ab')2 antibody prolong host survival in a murine xenograft model. *Cancer Res* 1991;51:5716–5721.
28. Rothenberg SP, daCosta M. Further observations on the folate-binding factor in some leukemic cells. *J Clin Invest* 1971;50:719–726.
29. Westerhof G R, Jansen G, van Emmerik N, et al. Membrane transport of natural folates and antifolate compounds in murine L1210 leukemia cells: role of carrier- and receptor-mediated transport systems. *Cancer Res* 1991;51:5507–5513.
30. Kamen BA, Capdevila A. Receptor-mediated folate accumulation is regulated by the cellular folate content. *Proc Natl Acad Sci USA* 1986;83:5983–5987.
31. Toffoli G, Cernigoi C, Russo A, Gallo A, Bagnoli M, Boiocchi M. Overexpression of folate binding protein in ovarian cancers. *Int J Cancer* 1977;74:193–198.
32. DuBeshter B, Lin J, Angel C, Poulter CA. Gynecologic tumors. In: Rubin P, ed. *Clinical oncology*, 7th ed. Philadelphia: WB Saunders; 1993:363–418.